Mechanical Stability and Charge Densities near Stacking Faults

J. M. MacLaren,[1] S. Crampin,[2] D. D. Vvedensky,[2] and M. E. Eberhart[3,4]
[1]*Theoretical Division, Los Alamos National Laboratory, Los Alamos, New Mexico 87545*
[2]*The Blackett Laboratory, Imperial College, London SW7 2BZ, United Kingdom*
[3]*Materials Science and Technology Division, Los Alamos National Laboratory, Los Alamos, New Mexico 87545*
[4]*Department of Materials Science and Engineering, Massachusetts Institute of Technology, Cambridge, Massachusetts 02139*
(Received 5 April 1988; revised manuscript received 30 January 1989)

The electronic structure near (111) twin stacking faults in Cu, Ir, and Al is investigated with the recently developed layer Korringa-Kohn-Rostoker method. The calculated stacking-fault energies are 341 mJ/m^2 (Ir), 118 mJ/m^2 (Al), and 58 mJ/m^2 (Cu), in excellent agreement with experiment. These trends are discussed in terms of changes in local bonding and symmetry at the stacking fault.

PACS numbers: 71.10.+x, 71.25.Cx, 73.20.−r, 73.40.−c

The relationship between electronic structure and mechanical properties of materials has received considerable attention, with emphasis on the development of atomistic models of fracture and deformation. However, quantum-mechanical modeling of mechanical behavior is confronted by several problems, including the complex origins of deformation processes, structural uncertainty, and a lack of computational techniques capable of yielding accurate information abut relevant structures such as complex interfaces. Nevertheless, there are examples where the microscopic origins of mechanical behavior has been identified and isolated in well-characterized systems.[1]

Most surface and interface electronic-structure calculations[2] have overcome the problems associated with reduced symmetry by utilizing thin-film or supercell structures incorporating the region of interest. However, in order to minimize the influence of the boundaries on interface electronic properties, more atoms may be required than for a corresponding calculation of the embedded structure. Alternative approaches involving embedding[3] and the incorporation of more realistic boundary conditions have been suggested by several authors.[4]

In this Letter we report a technique capable of performing accurate, first-principles calculations on structures such as stacking faults and grain boundaries. The method is based upon a layer Korringa-Kohn-Rostoker (LKKR) approach,[5] which can correctly describe the embedding of a planar defect in an otherwise perfect material. Within the LKKR framework the infinite solid is partitioned into layers of atoms, which are grouped into three regions: an interface region surrounded by two bulk regions. This partitioning allows the interface to be properly embedded, removing the need for slab or supercell boundary conditions. At present, the true crystal potential is replaced by an approximate muffin-tin form, and only the potentials in the interface layers are allowed to relax during the calculation.

The calculation of the self-consistent electronic structure proceeds by calculating the total Green's function G about each atom in a layer I embedded in left and right half spaces. The central quantity of interest is the local energy-resolved charge density $\rho(\mathbf{r};E)$, which is related in the usual way to the diagonal components of G in the coordinate representation, $\rho(\mathbf{r};E)=-(1/\pi)\mathrm{Im}G(\mathbf{r},\mathbf{r};E)$, from which the total charge density is obtained by an integration to the Fermi energy. G is evaluated by invoking the Dyson equation: $G=G_0+G_0TG_0$, where G_0 is the free-space Green's function and T is the scattering operator of the solid. The operator T may be written as $T=\tau_L+\tau_I+\tau_R$, where τ_I, τ_R, and τ_L sum all paths that end with scattering events in layer I, and the right and left half spaces adjacent to layer I, respectively. The τ obey "equations of motion" given in terms of the layer scattering operator T_I and the half-space reflectivities T_L^J and T_R^J of layers $J\rightarrow-\infty$ and $J\rightarrow\infty$, respectively, evaluated by application of layer-doubling and coupling algorithms.[5,6] For example,

$$\tau_L=T_L^{I-1}[1+G_0\tau_I+G_0\tau_R]\,, \tag{1}$$

with appropriate cyclic permutations for τ_I and τ_R. These equations may be solved for the τ in terms of the scattering operators, T, and G expressed as

$$G=G_0+G_0T_IG_0+G_0[1+T_IG_0]R^{\mathrm{eff}}[1+G_0T_I]G_0\,, \tag{2}$$

where

$$\begin{aligned}R^{\mathrm{eff}}=&[1-T_L^{I-1}G_0T_R^IG_0]^{-1}T_L^{I-1}[1+(1+G_0T_I)G_0T_R^{I+1}(1-G_0T_IG_0T_R^{I+1})^{-1}]\\&+[1-T_R^{I+1}G_0T_L^IG_0]^{-1}T_R^{I+1}[1+(1+G_0T_I)G_0T_L^{I-1}(1-G_0T_IG_0T_L^{I-1})^{-1}]\,.\end{aligned} \tag{3}$$

The first two terms in (2) represent the solution for an isolated layer and so provide the basis of a slab technique. The last term including the effective reflectivity R^{eff} of the surrounding solid provides the embedding of a semi-infinite medi-

um.

Within each layer the T_l may be expressed in terms of scattering-path operators τ^{ij} which sum all intralayer paths between atoms i and j of the layer: $T_l = \sum_{ij} \tau^{ij}$. The τ^{ij} also satisfy equations of motion:

$$\tau^{ij} = t^i \delta_{ij} + t^i \sum_k' (1 - \delta_{ik}) G_0 \tau^{kj}, \quad (4)$$

where t^i is the t matrix of atom i. Because of the two-dimensional periodicity, (4) may be solved by a Fourier transform.

A mixed basis set is used in the calculation of G, with an expansion in spherical waves for intralayer scattering by the muffin-tin potentials, and a plane-wave basis for interlayer scattering. This factorization of the scattering events facilitates a realistic treatment of complex interfaces, since the central-processor-unit time scales as $\sum_i n_i^3$, rather than as n_t^3, where n_i is the number of unique atoms in layer i, and $n_t = \sum_i n_i$ is the total number of unique atoms.

In practice iterative solutions for T_L^J and T_R^J are not uniformly convergent at real energies, near poles of the full Green's function. Thus, if at a specified real energy and parallel momentum there is an allowed three-dimensional Bloch state, then the iterative solution fails to converge; otherwise convergence is assured. Energy integrations are therefore performed along a contour in the complex plane which needs only to begin and end on the real axis to facilitate an application of the Cauchy residue theorem. The absorption introduced by the imaginary part of the energy means that the scattering sums converge after a finite number of layers have been included. In addition, since G is a smooth function at complex energy, the Brillouin zone and energy integrals needed for the charge-density and total-energy calculations can be accurately evaluated with only a few sampling points. For the muffin-tin density of states (MTDOS) presented below, the contour is offset 0.068 eV above the real energy axis.

The new potential is found from the calculated charge density as the sum of a Coulomb term, found from a solution of Poisson's equation for the interface geometry,[5] and an exchange-correlation contribution for which we adopt Slater's $X\alpha$ local-density approximation using tabulated values of α.[7] The procedure is then iterated to self-consistency, which for the present calculations required approximately 10–20 iterations to achieve the required accuracy in the total energy. These systems were iterated with a nine-layer interface, using $l = 2$ as the maximum angular momentum in the intralayer scattering, and thirteen plane waves for the interlayer scattering. The energy and **k** integrations were calculated with eight energy ordinates and six special **k** points[8] in the irreducible part of the Brillouin zone. Relativistic effects, important only in Ir, were included using the semirelativistic approach of Koelling and Harmon.[9] The densities of states were recalculated from the self-consistent potentials using 378 **k** points. These parameters gave good agreement between band structures and densities of states calculated with the LKKR code and other published results.[10]

As a first application the LKKR method is used to study twin faults in face-centered cubic (fcc) metals. An understanding of the electronic origins of the stacking-fault energy is crucial to the development of a general theory of mechanical behavior. Materials with low stacking-fault energies are characterized by planar slip and twin formation, while those with high stacking-fault energies are characterized by more homogeneous deformation and dislocation cell formation due to easy cross slip.[11] The calculations reported below are for a twin-stacking-fault structure constructed by altering the fcc stacking sequence along the [111] direction to the locally hexagonal close-packed sequence at the interface, i.e., from the fcc ... *ABCABCABC* ... to the ... *ABCA-BACBA* ... sequence.

The three metals we study are Ir, an unusual fcc material, having a tendency to cleave as well as fail intergranularly and, despite a very high stacking-fault energy, reported to exhibit deformation twinning;[12] Al, a high-stacking-fault-energy material not showing any deformation twins; and Cu, a comparatively low-stacking-fault-energy material characterized by deformation twins under shock loading. The anomalous fracture behavior of Ir has been suggested[12] to arise from the increased d contribution to the cohesive energy in comparison with other fcc metals as evidenced, for example, by the relatively wide (6 eV) d band and relatively narrow (2 eV) occupied part of the s band.

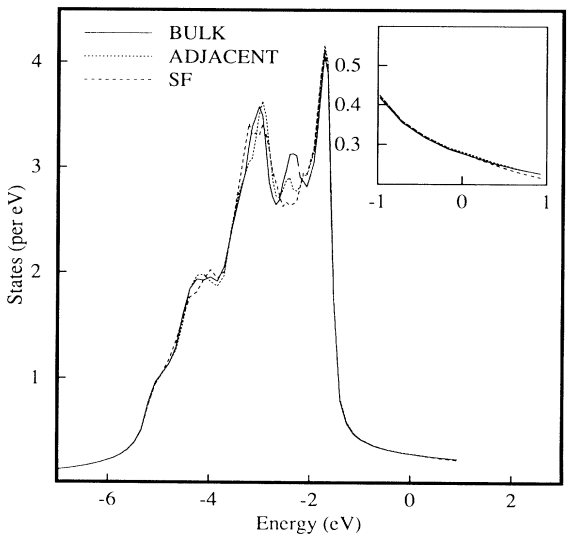

FIG. 1. MTDOS for atoms near a Cu stacking fault. The zero of energy is at the Fermi energy. Shown are the densities of states for the stacking-fault (SF) layer, the adjacent layer, and the bulk. Inset: The Fermi-energy densities of states.

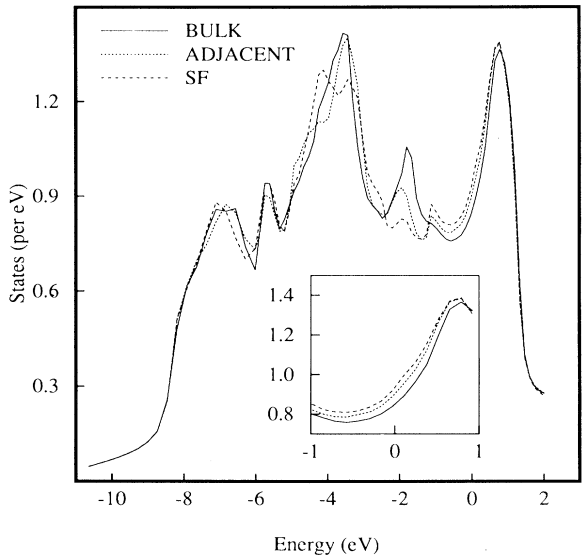

FIG. 2. Same as Fig. 1 for Ir.

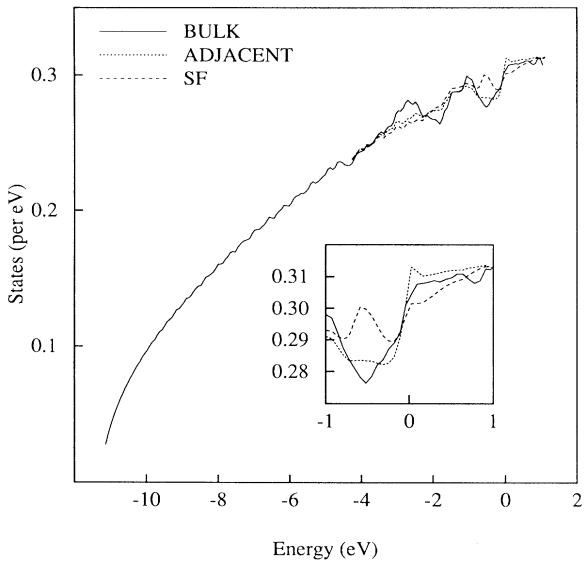

FIG. 3. Same as Fig. 1 for Al.

Shown in Fig. 1 is the MTDOS for atoms near the Cu stacking fault. The changes in the total MTDOS induced by the structural perturbation are evidently small, and found primarily within the *d* bands. The MTDOS at the Fermi energy is unaffected, being dominated by *s* and *p* contributions, which are spatially diffuse and are therefore able to accommodate the local changes in environment. The changes in the *d* band are due primarily to changes in the hybridization and the splitting of some of the *d*-band peaks resulting from the local mirror symmetry at the fault.

Figure 2 shows the corresponding result for Ir. The perturbations are seen to extend throughout the band and are clearly much larger than in Cu. In particular, the MTDOS is enhanced by approximately 7% at the Fermi level, which lies within the *d* band, where there is a relatively small *sp* contribution in comparison with Cu.

In Figure 3 we present the results for the Al stacking fault. The changes occur predominantly around the Fermi energy, but are much less localized at the fault than in Cu and Ir where the perturbations only extend three layers away from the fault. This reflects the weaker scattering power of the Al atoms, producing a longer electron mean free path. The induced mirror symmetry at the stacking fault is important in Al due to inhibited hybridization between *s* and *p* electrons.

Many of the local changes in the MTDOS shown in Figs. 1–3 can be explained qualitatively in terms of the influence upon hybridization of the symmetry induced by the fault. In Table I we show the partial-wave components of the occupied bands along the [111] direction in Ir, Al, and Cu and the associated parity under reflection through a plane perpendicular to the [111] direction, which is appropriate for the stacking-fault layer. In the perfect fcc crystal both even and odd components can hybridize. In Cu, the Λ_1 band has a comparatively small *p* component, so the stacking fault induces a much smaller perturbation than in the Λ_3 band, where two types of *d* levels are split. In Al, for which there is no occupied Λ_3 band, the second branch of the Λ_1 band is significantly perturbed due to the inhibited *sp* hybridization. Finally, for Ir, with relatively wide *d* bands, the Λ_3 band is considerably more perturbed than in Cu.

The fault energies have been calculated by taking the difference between total energies of the perfect crystal and of the system with an isolated stacking fault. We find 341 mJ/m^2 for Ir, 118 mJ/m^2 for Al, and 58 mJ/m^2 for Cu. The calculated values are in good agreement with published fault energies: Ir, 300 mJ/m^2;[13] Al, 166 mJ/m^2;[13] and Cu, 45 mJ/m^2,[14] 78 mJ/m^2.[13] These experimental values are determined indirectly from isotropic elasticity theory combined with field-ion-microscope measurements on dislocation structure. Both elasticity theory and microscopy give rise to errors which cannot be corrected.[13] The calculated stacking-fault energies also have uncertainties due to numerical errors arising from the small value of the stacking-fault energy, from the muffin-tin approximation, and from the lack of structural relaxation. However, the values do reproduce

TABLE I. The parity under reflection through a (111) plane of the lowest partial-wave contributions to the indicated bands along the [111] direction in an fcc material.

Parity under reflection	Λ_1	Λ_3
Even	*s*,*d*	*p*,*d*
Odd	*p*	*d*

the experimental trend and can be systematically improved. These facts, coupled with the importance of stacking-fault energies for an understanding of deformation behavior, point to the need for calculational techniques that can determine quantities inaccessible to experiment.

This work was supported by the (U.K.) Science and Engineering Research Council, the (U.S.) Department of Energy, and by a NATO travel grant. J.M.M. acknowledges useful discussions with M. E. McHenry and R. C. Albers.

[1]S. G. Roberts, P. Pirouz, and P. B. Hirsch, J. Mater. Sci. **20**, 1739 (1985).

[2]M. Posternak, H. Krakauer, A. J. Freeman, and D. D. Koelling, Phys. Rev. B **21**, 5601 (1980); D. P. Di Vincenzo, O. L. Alerhand, M. Schlüter, and J. W. Wilkins, Phys. Rev. Lett. **56**, 1925 (1986); M. Y. Chou, M. L. Cohen, and S. G. Louie, Phys. Rev. B **32**, 7979 (1986); E. Wimmer, C. L. Fu, and A. J. Freeman, Phys. Rev. Lett. **55**, 2618 (1985).

[3]J. E. Inglesfield, Phys. Rev. B **37**, 6682 (1988).

[4]F. Maca and M. Scheffler, Comput. Phys. Commun. **38**, 403 (1985); A Gonis, Phys. Rev. B **34**, 8313 (1986); G. Wachutka, Phys. Rev. B **34**, 8512 (1986).

[5]J. M. MacLaren, S. Crampin, D. D. Vvedensky, and J. B. Pendry, Phys. Rev. B (to be published).

[6]J. B. Pendry, *Low Energy Electron Diffraction* (Academic, London, 1974).

[7]K. Schwarz, Phys. Rev. B **5**, 2466 (1972). For Ir, a value of $\alpha=0.7$ was used.

[8]S. I. Cunningham, Phys. Rev. B **10**, 4988 (1971).

[9]D. D. Koelling and B. N. Harmon, J. Phys. C **10**, 3107 (1977).

[10]V. L. Moruzzi, J. F. Janak, and A. R. Williams, *Calculated Electronic Properties of Metals* (Pergamon, New York, 1978).

[11]J. P. Hirth and J. Lothe, *Theory of Dislocations* (Wiley Interscience, New York, 1982).

[12]S. S. Hecker, D. L. Rohr, and D. F. Stein, Metall. Trans. **9A**, 481 (1978); D. L. Rohr, L. E. Murr, and S. S. Hecker, Metall. Trans. **10A**, 399 (1979).

[13]L. E. Murr, *Interfacial Phenomena in Metals and Alloys* (Addison-Wesley, Reading, MA, 1975).

[14]C. B. Carter and I. L. F. Ray, Philos. Mag. **35**, 1161 (1977).